Carbohydrate Polymers 83 (2011) 452–461

Contents lists available at ScienceDirect

Carbohydrate Polymers

journal homepage: www.elsevier.com/locate/carbpol

Efficient water soluble *O*-carboxymethyl chitosan nanocarrier for the delivery of curcumin to cancer cells

A. Anitha [a], S. Maya [a], N. Deepa [a], K.P. Chennazhi [a], S.V. Nair [a], H. Tamura [b], R. Jayakumar [a,*]

[a] *Amrita Centre for Nanosciences and Molecular Medicine, Amrita Institute of Medical Sciences and Research Centre, Amrita Vishwa Vidyapeetham University, Kochi 682041, India*
[b] *Faculty of Chemistry, Materials and Bioengineering, Kansai University, Osaka 564-8680, Japan*

ARTICLE INFO

Article history:
Received 16 July 2010
Received in revised form 29 July 2010
Accepted 2 August 2010
Available online 11 August 2010

Keywords:
Carboxymethyl chitosan
Curcumin
Nanoformulation
Drug delivery
Cytotoxicity
Cellular uptake

ABSTRACT

Carboxymethyl chitosan derivatives are widely used for biomedical applications because of their non-toxic and biodegradable properties. Curcumin is a phytochemical with immense biological properties. But its hydrophobicity and poor oral bioavailability limits its application as a chemotherapeutic agent. To increase the oral bioavailability, we developed curcumin loaded *O*-CMC nanoparticles (curcumin-*O*-CMC Nps). The prepared nanoparticles were characterized by DLS, AFM, SEM, FT-IR, XRD and TG/DTA. Size analysis studies revealed spherical particles with mean diameter of about 150 ± 30 nm. Curcumin was entrapped in *O*-CMC with an efficiency of 87%. *In vitro* drug release profile was studied at 37 °C under different pHs (7.4 and 4.5) with and without lysozyme. Cytotoxicity studies by MTT assay indicated that curcumin-*O*-CMC Nps were toxic to cancer and non-toxic to normal cells. Cellular uptake of the curcumin-*O*-CMC Nps was analyzed by fluorescence microscopy and FACS. Overall these studies indicated *O*-CMC as a promising nanomatrix for drug delivery applications.

1. Introduction

Nanotherapeutics, a hot-spot in the field of medicine, especially nanoparticle based drug delivery for cancer therapy is spreading rapidly which can overcome the limitations of conventional drug delivery systems. Nanometric drug carriers of optimum size and surface characteristics are highly stable and possess high carrying capacity. Moreover the feasibility of incorporation of both hydrophilic and hydrophobic substances and feasibility of variable routes of administration allow controlled drug release from the matrix and improved drug bioavailability (Gelperina, Kisich, Iseman, & Heifets, 2005; Jung et al., 2000).

Chitosan is a natural polysaccharide obtained from crustacean shells and is composed of 2-amino-2-deoxy-β-D-glucan combined with glycosidic linkages. The primary amine groups render special properties that make chitosan very useful in pharmaceutical applications. The non-toxicity, biodegradability and biocompatibility makes chitosan suitable for various biomedical applications such as drug delivery (Dev et al., 2010; Khan, Peh, & Chng, 2000; Mathew et al., 2010; Rabea, Badawy, Stevens, Smagghe, & Steubaut, 2003), gene delivery (Csaba, Koping-Hoggard, & Alonso, 2009; Jayakumar et al., 2010), wound dressing (Jayakumar, Nair, & Tamura, 2009; Madhumathi et al., 2010; Sudheesh Kumar et al., 2010; Wang, Du, Fan, Liu, & Hu, 2005) and tissue engineering (Khor and Lim, 2003; Peter et al., 2010). The potential application of chitosan is hindered by its limited solubility in aqueous media. Thus, chitosan is chemically modified so as to improve the polymer processability, solubility, antimicrobial activity and the ability to interact with other substances (Jayakumar et al., 2010). Introducing a carboxymethyl group is the most advantageous method of increasing the solubility of chitosan at neutral and alkaline pH without affecting other important characteristics. The reaction carried out at room temperature favors *O*-substitution and higher temperature favors *N*-substitution which is indicative that temperature is a critical factor in carboxymethylation of chitosan (Fernando & Sergio, 2004). *O*-CMC is an amphiprotic ether derivative of chitosan, containing –COOH and $–NH_2$ groups in the molecule and exhibit non-toxicity, biodegradability, biocompatibility, antibacterial, and antifungal activity and has therefore received considerable attention in biomedical applications (Muzzarelli et al., 1998; Jayakumar et al., 2010). *O*-CMC can be prepared by reacting chitosan with monochloroacetic acid in isopropyl alcohol as a solvent at room temperature (Anitha et al., 2009; Chen & Park, 2003; Liu, Guan, Yang, Li, & Yao, 2001). Many pharmaceutical companies are increasingly interested in developing multi-targeted therapies. Plant-based products, however, accomplish multi-targeting naturally and, in addition, are inexpensive and safe compared to synthetic agents.

Curcumin is a hydrophobic polyphenol derived from turmeric, the rhizome of the herb *Curcuma longa*. Chemically, it is a bis-α, β-unsaturated β-diketone (commonly called diferuloylmethane) that

* Corresponding author. Tel.: +91 484 2801234; fax: +91 484 2802020.
E-mail addresses: rjayakumar@aims.amrita.edu, jayakumar77@yahoo.com (R. Jayakumar).

0144-8617/$ – see front matter © 2010 Elsevier Ltd. All rights reserved.
doi:10.1016/j.carbpol.2010.08.008

exhibits keto-enol tautomerism, having a predominant keto form in acidic and neutral solutions and a stable enol form in alkaline media (Anand et al., 2008).

Curcumin exhibit immense biological properties like antioxidant, anti-inflammatory, antimicrobial and anticarcinogenic activities, hepato and nephro protective, regulates various immune cells like T lymphocytes (CD4 and CD8), B lymphocytes, natural killer cells, macrophages, dendritic cells and other immune cells, regulates multiple targets (multi-targeted therapy), which is needed for the treatment of most diseases, and it is inexpensive and has been found to be safe in human clinical trials (Lao, Demierre, & Sondak, 2006; Qureshi, Shah, & Ageel, 1992; Shankar, Shantha, Ramesh, Murthy, & Murthy, 1980; Li, Ahmed, Mehta, & Kurzrock, 2007).

Despite these promising features a major drawback with curcumin is its extremely low solubility in aqueous solutions, which limits its bioavailability and clinical efficacy. It degrades by acidic and alkaline hydrolysis, oxidation and photodegradation. The decomposition occurs in a pH dependant manner, with faster reactions at neutral to basic conditions. They are known to be stable at a pH < 6.5 (Pfeiffer, Hohle, Solyom, & Metzler, 2003; Wang, Pan, Cheng, Lin, & Lin, 1997). Different studies of curcumin have shown poor absorption, rapid metabolism, and elimination of curcumin as the major reasons for poor bioavailability of this extremely beneficial polyphenolic compound to mankind (Mishra, Mohammada, & Mishra, 2008). To increase its aqueous solubility and bioavailability, attempts have been made to encapsulate the drug in polymeric micelles (Muller & Keck, 2004), solid lipid nanoparticles (Tiyaboonchai, Tungpradit, & Plianbangchang, 2007), polymeric nanoparticles (Karikar et al., 2007), biodegradable microspheres (Kumar et al., 2002), phospholipids (Sou, Inenaga, Takeoka, & Tsuchida, 2007) cyclodextrin (Salmaso, Bersani, Semenzato, & Caliceti, 2007), hydrogel (Vemula, Li, & John, 2006) and liposomes (Li et al., 2007).

The present study aims in evaluating the ability of *O*-CMC as a carrier for hydrophobic drugs in cancer drug delivery applications. We report a simple method of solvent evaporation followed by ionic gelation to develop a nanoformulation based on *O*-CMC into which the hydrophobic anticancer drug, curcumin was loaded. This approach has tried to solubilize curcumin and there after to stabilize curcumin in *O*-CMC Nps. Drug loaded Nps were obtained easily under mild conditions. The Nps were non-toxic and compatible towards normal cells whereas enhanced cellular uptake resulted in comparable anticancer effects similar to that of free curcumin towards cancer cell. Overall, *O*-CMC Nps proved to be an efficient carrier for the controlled delivery of anticancer drugs like curcumin to cancer cells.

2. Materials and methods

2.1. Materials

O-CMC (degree of deacetylation 61.8% and degree of substitution 0.54) was purchased from Koyo chemical Co. Ltd., Japan, calcium chloride ($CaCl_2$), cell culture media like minimum essential medium (MEM) and Dulbecco's modified eagle medium (DMEM) and MTT [3-(4,5-Dimethylthiazole-2-yl)-2,5-diphenyl tetrazolium] was purchased from Sigma–Aldrich, curcumin was purchased from Merck, mouse fibroblast cells (L929), human breast cancer cell line (MCF-7) and human prostate cancer cell line (PC-3) for cell culture experiments was purchased from NCCS, Pune. All other chemicals used were of analytical grade.

2.2. Methods

2.2.1. Preparation of O-CMC nanoparticles

O-CMC Nps were prepared by the ionic cross-linking reaction of *O*-CMC with $CaCl_2$ as described in literature (Anitha et al., 2009; Shi, Du, Yang, Zhang, & Sun, 2006). 0.05 wt% *O*-CMC solution was prepared in distilled water. To 10 ml of this solution, 1 ml of 1 wt% $CaCl_2$ solution was added under constant stirring. As a result the clear solution changed into an opalescent suspension. The resulting Nps were purified by centrifugation at 20,000 rpm for 45 min. The pellet was washed, redispersed in distilled water and lyophilized. The lyophilized sample was used for further characterization and studies.

2.2.2. Preparation of curcumin loaded O-CMC nanoparticles

A stock solution of curcumin was prepared in ethanol at a concentration of 2 mg/ml. 10 mg *O*-CMC was dissolved in 20 ml millipore water under stirring. Curcumin was loaded into *O*-CMC solution by adding required volume of curcumin solution drop wise under continuous stirring for 30 min. 1 wt% $CaCl_2$ was added to the polymer solution and stirred for an hour resulting in the formation of curcumin-*O*-CMC Nps.

2.2.3. Nanoparticle size analysis and stability studies

The size distribution of *O*-CMC Nps before and after drug loading was analyzed by dynamic light scattering (DLS using DLS-ZP/Particle Sizer Nicomp ™380 ZLS). The average size and surface morphology of the Nps were further analyzed by atomic force microscopy (AFM) using JEOL JSPM-5200 and scanning electron microscopy (SEM) using JEOLJSM-6490LA. For SEM and AFM the Np suspension was diluted 10-fold with millipore water and a drop was placed on a metallic stub and freshly prepared mica sheet pasted AFM stub, then the sample was air dried and scanned. Surface charge and thereby the stability of Np system was obtained by zeta potential measurements (DLS-ZP/Particle Sizer Nicomp ™380 ZLS).

2.2.4. Nanoparticle characterizations

The potential interaction between the constituents within the Np system was analyzed by Fourier transform infrared (FT-IR) spectroscopy. FT-IR spectra of *O*-CMC, curcumin, *O*-CMC Nps and curcumin-*O*-CMC Nps were recorded on Perklin Elmer Spectrum RXI Fourier Transform Infrared spectrophotometer using KBr method. To understand the physical nature of curcumin in the curcumin-*O*-CMC Nps, X-ray diffraction (XRD) analysis was done by PAN analytical X'Pert PRO X-ray diffractometer. Thermal behavior of *O*-CMC, curcumin and curcumin-*O*-CMC Nps were studied through thermogravimetry and differential thermal analysis (TG/DTA) using SII TG/DTA 6200 EXSTAR.

2.2.5. Entrapment efficiency and loading efficiency

To determine the entrapment efficiency of curcumin within *O*-CMC Nps, it was first separated by ultra-centrifugation at 20,000 rpm at 4 °C for 45 min from the aqueous medium containing free curcumin. The pellet was washed twice with distilled water and then redispersed in ethanol, vortexed well and centrifuged. The yellowish supernatant was collected and quantified spectrophotometrically at 429 nm. Loading efficiency of the system was also calculated with respect to the weight of the Nps obtained after centrifugation (Kim et al., 2006; Das, Kasoju, & Bora, 2010).

$$\text{Entrapment efficiency}\,(\%) = \frac{\text{Total amount of curcumin} - \text{free curcumin}}{\text{Total amount of curcumin}} \times 100$$

$$\text{Loading efficiency}\,(\%) = \frac{\text{Total amount of curcumin}}{\text{Total amount of nanoparticles}} \times 100$$

2.2.6. In vitro drug release studies

In vitro curcumin release profiles from *O*-CMC Nps were determined at pH 7.4 and 4.5. The Np suspension was centrifuged at 20,000 rpm for 45 min and the collected pellet was redispersed in 10 ml of phosphate-buffered saline solution (pH 7.4 and 4.5) at a final concentration of 0.2 mg/ml. Release was also studied in the presence of lysozyme at a concentration of 1 mg/ml. Total volume was divided into 20 eppendorf tubes with 0.5 ml each for a period of one week. The tubes were incubated at 37 °C under gentle shaking. At proper time intervals, curcumin in Nps was first extracted in ethanol and quantified spectrophotometrically. Release was quantified as follows (Das et al., 2010).

$$\text{Release}\,(\%) = \frac{\text{Released curcumin}}{\text{Total curcumin}} \times 100$$

2.2.7. Cell culture

For cell culture experiments L929, MCF-7 and PC-3 cell lines were used. L929 and MCF-7 were maintained in MEM and PC-3 was maintained in DMEM supplemented with 10% fetal bovine serum (FBS). The cells were incubated in CO_2 incubator at 37 °C with 5% CO_2. After reaching confluency, the cells were detached from the flask with Trypsin-EDTA. The cell suspension was centrifuged at 3000 rpm for 3 min and then resuspended in the growth medium for further experiments.

2.2.8. Cytotoxicity studies

For cytotoxicity experiments, cells were seeded at a density of 10,000 cells/well into a 96 well plate. MTT assay was performed to evaluate cytotoxicity of the prepared Nps and this is a colorimetric test based on the selective ability of viable cells to reduce the tetrazolium component of MTT in to purple colored formazan crystals. Five different concentrations of the curcumin-*O*-CMC Nps (1, 2, 3, 4 and 5 mg/ml) were prepared by dilution with the media. After reaching 90% confluency, the cells were incubated with different concentrations of the Nps (100 μl) for a period of 24 h. Cells in media alone devoid of Nps acted as negative control and wells treated with Triton X-100 as positive control. The cells were incubated with MTT solution for 4 h followed by 1 h incubation with solubilization buffer. The optical density of the solution was measured at a wavelength of 570 nm using a Beckmann Coulter Elisa plate reader (BioTek Power Wave XS). Triplicate samples were analyzed for each experiment. Cell viability was expressed as the percentage of the negative control calculated as

$$\text{Viability}\,(\%) = \frac{\text{Nt}}{\text{Nc}} \times 100$$

Nt is the optical density of cells treated with sample and Nc is the absorbance of the untreated cells.

2.2.9. Cell uptake studies

Cell uptake studies of the prepared *O*-CMC Nps and curcumin-*O*-CMC Nps were studied by fluorescent imaging. For this acid etched cover slips were kept in 24 well plates and were seeded with 10,000 cells per cover slip and incubated for 24 h for the cells to attach on the cover slips. After 24 h incubation, the media was removed and the wells were carefully washed with PBS buffer. Then the drug loaded *O*-CMC Nps suspension at a concentration of 1 and 5 mg/ml was added along with the media to triplicate wells and incubated for 24 h. Thereafter the cover slips were processed for imaging using fluorescent microscopy. The processing involved washing the cover slips with PBS and thereafter fixing the cells in 5% para formaldehyde followed by a final PBS wash. The cover slips were air dried and mounted on to glass slides with DPX as the mountant medium. The slides were then viewed under the fluorescence microscope.

2.2.10. Cell uptake measurements by UV quantification

The absorption spectrum of curcumin in the cell lysate gives a comparative account of the amount taken up by normal cells and cancer cells. Cells (L929 and MCF-7) were seeded into a 24 well plate with a density of 10,000 cells per well and after the cells reached 90% confluency, curcumin-*O*-CMC Nps of 1 mg/ml concentration in media was added to the cells. After 1, 6, 12, 24 and 48 h incubation, the cells were washed with PBS and trypsinized. The cells were lysed with ethanol under sonication and the internalized particles were extracted. The lysate was centrifuged for 10 min at 10,000 rpm and supernatant containing ethanolic curcumin was quantified spectrophotometrically at 429 nm (Kunwar et al., 2008).

2.2.11. Cellular uptake by flow cytometry

The cellular uptake of curcumin-*O*-CMC Nps by the normal and cancer cells were confirmed by Fluorescence Activated Cell Sorting (FACS) analysis. Cells were seeded in a 24 well plate at a density of 50,000 cells/well. After reaching 90% confluency, different concentrations of the Nps (1 and 5 mg/ml) were added and incubated at 37 °C for 24 h. Intra cellular curcumin fluorescence was analyzed flow cytometrically after excitation with a 488 nm argon laser using FACS Aria II (Beckton and Dickinson, Sanjose, CA). Fluorescence emission above 530 nm from 10,000 cells were collected, amplified and scaled to generate single parameter histogram.

2.2.12. Apoptosis assay by flow cytometry

The Phosphatidyl serine (PS) exposure in both L929 and MCF-7 cells were detected using an Annexin V-FITC/PI Vybrant apoptosis assay kit (Molecular probes, Eugene, OR). After reaching 90% confluency the cells were treated with 1 and 5 mg/ml of curcumin-*O*-CMC Nps as described previously and incubated for 24 h. Cells were trypsinized and washed with ice-cold PBS for 5 min at 500 g at 4 °C. The supernatant was discarded and the pellet was resuspended in ice-cold 1X Annexin binding buffer (5×10^5 to 5×10^6 cells/ml). 5 μl of Annexin V-FITC solution and 1 μl of PI (100 μg/ml) were added to 100 μl of the cell suspensions. The samples were mixed gently and incubated at room temperature for 15 min in the dark. After incubation, 400 μl of ice-cold 1X binding buffer was added and mixed gently, and analyzed by flow cytometry. Cells in media alone devoid of Nps (negative control) and cells treated with *O*-CMC Nps were also analyzed in the same way.

3. Results and discussion

3.1. Preparation of O-CMC and curcumin loaded O-CMC nanoparticles

O-CMC Nps were prepared by the ionic cross linking between carboxyl group of *O*-CMC with Ca^{2+} ions of $CaCl_2$ (Anitha et al., 2009; Shi et al., 2006). The major factors that had critical effects on nanoparticle formation include concentration of the polymer and cross linker and stirring speed. Nanoformulation also enhanced the solubility of curcumin. From Fig. 1C it can be clearly observed that curcumin as such is insoluble in water whereas Np suspension with loaded curcumin enhances drug solubility.

3.2. Nanoparticle size and morphology

The size distribution of *O*-CMC and curcumin-*O*-CMC Nps were obtained using DLS (Fig. 2(A and B)) which showed that *O*-CMC Nps lies within a size range of 70–100 nm and curucmin-*O*-CMC Nps lies within 120–180 nm.

The size and morphology of the Nps were reconfirmed by AFM and SEM. Fig. 2(C and D) displays the AFM images of *O*-CMC and curcumin-*O*-CMC Nps, showing uniformly sized spherical particles with a mean size of 100 ± 20 and 150 ± 30 nm, respectively. Fig. 2(E)

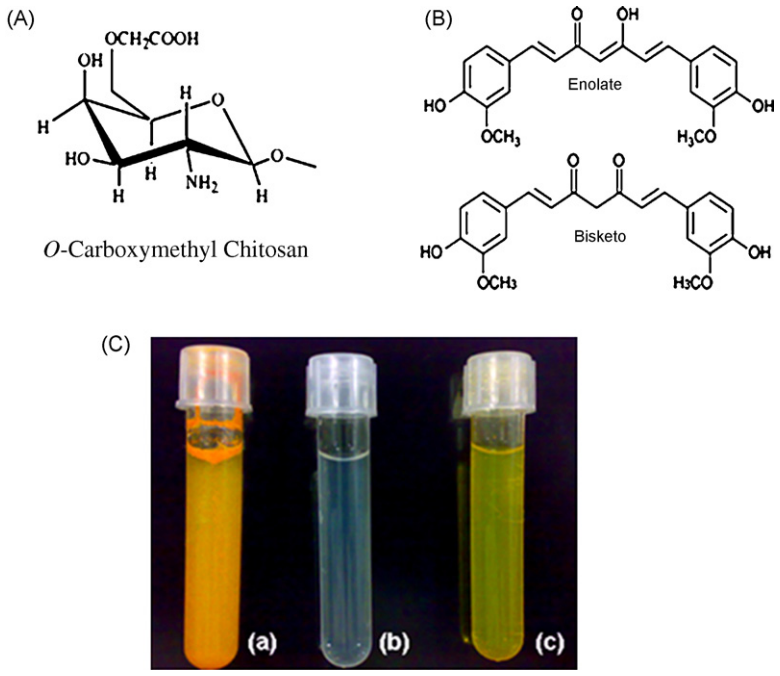

Fig. 1. (A) Chemical structure of *O*-CMC (B) Chemical structure of curcumin (C) Solubility of curcumin (a) curcumin in water (b) *O*-CMC Nps (c) curcumin-*O*-CMC Nps.

displays the SEM images of curcumin-*O*-CMC Nps indicating spherical particles within a size range of 200 nm. For delivering the drug via Nps, their size should be tuned in such a way that the Nps should be large enough to prevent rapid leakage into blood capillaries but escape the capture by macrophages lodged in the reticuloendothelial system (Cho, Wang, Nie, Chen, & Shin, 2008). Curcumin-*O*-CMC Nps lies in the optimal size range (below 200 nm) suitable for drug delivery applications.

3.3. Zeta potential measurements

From zeta potential measurements, the stability of the Nps system was evaluated. For *O*-CMC and curcumin-*O*-CMC Nps, the zeta potential value was found to be −35.12 and −30 mV that lies in the stable range indicating that the prepared Nps systems were stable. The negative surface charge of both *O*-CMC and curcumin-*O*-CMC Nps can be attributed to the presence of COO^- groups and

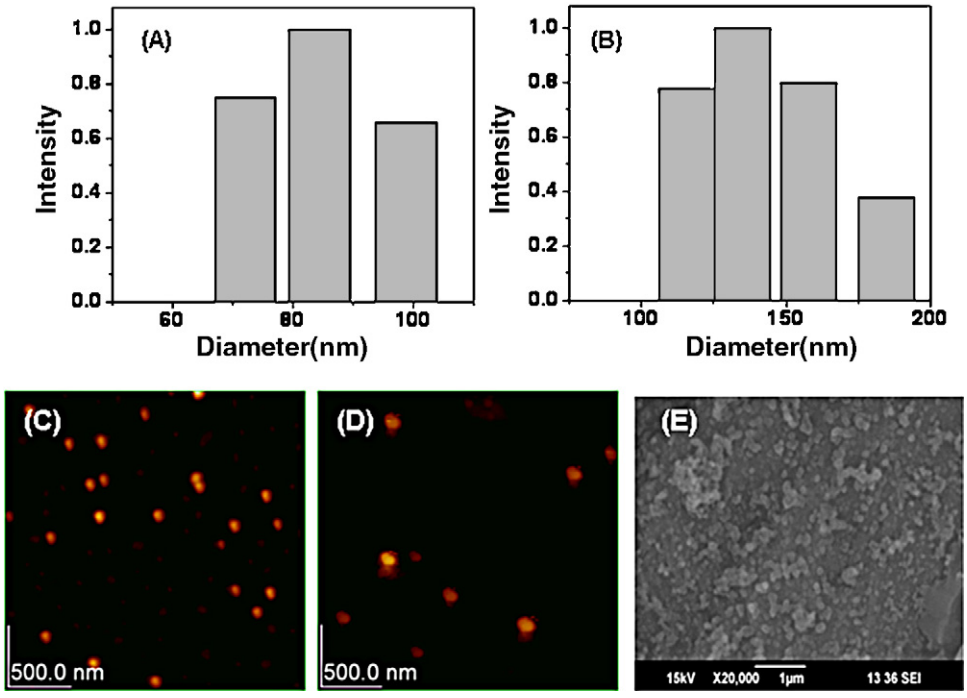

Fig. 2. (A) and (B) Particle size distribution of *O*-CMC and curcumin-*O*-CMC Nps by DLS (C) and (D) AFM image of *O*-CMC and curcumin-*O*-CMC Nps (E) SEM image of curcumin-*O*-CMC Nps.

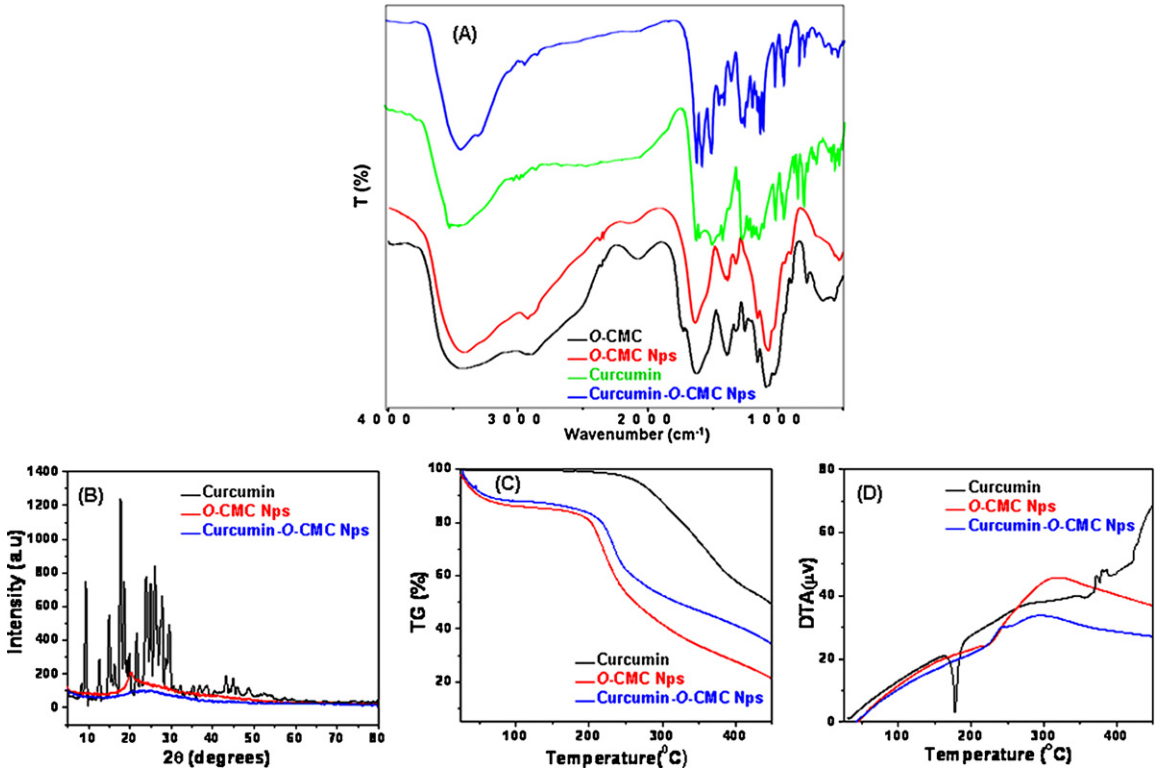

Fig. 3. (A) FT-IR spectrum showing *O*-CMC, *O*-CMC Nps, curcumin and curcumin-*O*-CMC Nps (B) XRD pattern (C) TGA curve (D) DTA curve showing curcumin, *O*-CMC and curcumin-*O*-CMC Nps.

the reduction in surface charge after loading of curcumin can be explained based on hydrogen bonding between the carboxyl group of *O*-CMC and hydroxyl group of curcumin.

3.4. Nanoparticle characterizations

3.4.1. FT-IR

FT-IR spectroscopy was performed to ascertain the formation of curcumin-*O*-CMC Nps. Fig. 3A shows the FT-IR spectrum of *O*-CMC, *O*-CMC Nps, curcumin and curcumin-*O*-CMC Nps. The FT-IR spectrum of *O*-CMC, showed broad band at 3420 cm^{-1} due to the stretching vibrations of amine and hydroxyl groups. Peaks at 1740 and 1629 cm^{-1} corresponds to the stretching vibrations of carbonyl and protonated amino groups and a strong peak at 1320 cm^{-1} is due to C–O stretching. In nanoparticles formulation, no absorption band was found in the region of 1740 cm^{-1} and the presence of strong band appeared at 1639 cm^{-1} and less intense peak at 1320 cm^{-1} which can be attributed to the stretching vibrations of calcium cross-linked carboxyl groups of *O*-CMC (Anitha et al., 2009; Zhuang & Liu, 2006).

The FT-IR spectrum of curcumin exhibited an absorption band at 3510 cm^{-1} attributed to the phenolic O–H stretching vibration. Additionally, sharp absorption bands at 1605 cm^{-1} (stretching vibrations of benzene ring), 1502 cm^{-1} (C=O and C–C vibrations), 1435 cm^{-1} (olefinic C–H bending vibration) and 1285 cm^{-1} (aromatic C–O stretching vibration) (Yallapua, Jaggi, & Chauhana, 2010). Because of the complexation of curcumin with the *O*-CMC Nps, the wave numbers corresponding to the characteristic peaks of *O*-CMC was shifted. Comparing *O*-CMC and drug loaded *O*-CMC Nps peak shifts were observed from 3429 to 3284 cm^{-1} and 1639 to 1627 cm^{-1}. This data confirmed the presence of curucmin in the *O*-CMC Np matrices.

3.4.2. XRD

To understand the physical nature of curcumin with in the Nps, XRD pattern (Fig. 3B) of pure curcumin, *O*-CMC Nps and curcumin-*O*-CMC Nps were compared. Curcumin displayed the characteristic crystalline peaks of 2θ between 20° and 30°. *O*-CMC being amorphous did not show any peaks. However, curcumin-*O*-CMC Nps exhibited no such crystalline peaks, possibly due to the formation of an amorphous complex which can be attributed to the intermolecular interaction between *O*-CMC and curcumin within the Np matrix (Shaikh, Ankola, Beniwal, Singh, & Ravikumar, 2009; Yallapua et al., 2010).

3.4.3. Thermal studies

TGA studies of curcumin, *O*-CMC and curcumin-*O*-CMC Nps were done to study their thermal behavior. Fig. 3C shows the degradation of curcumin, *O*-CMC and curcumin-*O*-CMC Nps with temperature. Within 100 °C weight reduction can be due to moisture loss. TG curve clearly indicates curcumin degrades in a slower rate and at 450 °C, curcumin is degraded only 50%, whereas the *O*-CMC is degraded to 20% at this temperature. This data shows that curcumin-*O*-CMC Nps showed an improved thermal stability compared to *O*-CMC due to the presence of curcumin. In particular, complexation of a drug and a polymer results in the absence/shifting of endothermic peaks, indicating a change in the crystal lattice, melting, boiling, or sublimation points (Yallapua et al., 2010). The amorphous nature of curcumin, loaded in the Nps was reconfirmed by DTA (Fig. 3D). The DTA curve shows an endothermic peak at 200 °C for crystalline curcumin which disappeared in curcumin-*O*-CMC Nps. This behavior confirms amorphous nature of curcumin with in *O*-CMC Nps.

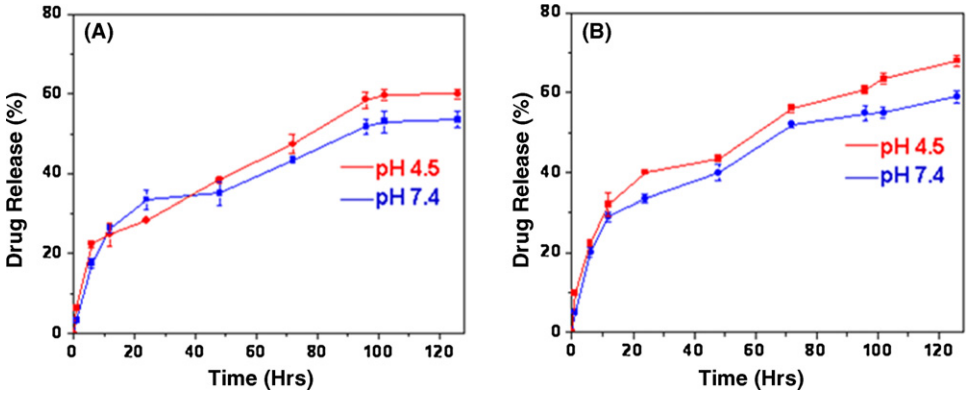

Fig. 4. Drug release profile of curcumin from *O*-CMC Nps (A) without lysozyme (B) with lysozyme at two different pHs 4.5 and 7.4.

3.5. Determination of entrapment efficiency and loading efficiency

The main focus of the study was to develop a better carrier for curcumin and the technique followed here facilitate the loading and entrapment of different amounts of curcumin into *O*-CMC Nps. Entrapment and loading efficiency of curcumin in *O*-CMC Nps was found to be 87% and 48%, respectively. Experimental results indicated that the concentration of the *O*-CMC and curcumin had critical effects on the drug loading. Higher amount of *O*-CMC allows more loading and entrapment, but resulted in large sized particles. At higher drug concentration entrapment efficiency was reduced where the drug tends to precipitate. Considering all these factors, concentration of *O*-CMC and curcumin was optimized so as to give better entrapment, loading efficiency and desired size.

3.6. In vitro drug release

Fig. 4 shows the release profile of curcumin from *O*-CMC Nps at two different pHs (4.5 and 7.4) and also with and without lysozyme. Initially the drug is released in a very slow controlled manner and finally becomes sustained.

From the drug release curve it is clear that at the 12th h there was a 24% and 26% curcumin release from *O*-CMC matrix which reaches 53% and 59% at pH 7.4 and 4.5 respectively after 6 days (Fig. 4A). The pH dependant release can be attributed to the swelling property of the polymer matrix. At lower pH the residual amine groups is protonated and creates a repulsive force between the adjacent positive charge thereby causing the polymer to swell and more amount of drug will be diffused out. Basic medium, unlike acidic medium limits its swelling which inhibits the diffusion of drugs at a faster rate (Prabaharan, Reis, & Mano, 2007).

In the presence of lysozyme (Fig. 4B) release of the drug from the nanoparticle matrix was enhanced as a result of which 59% (pH 7.4) and 68% (pH 4.5) curcumin was released after 6 days. Lysozyme acts on chitosan and its derivatives by hydrolyzing glucosamine-glucosamine, glucosamine-N-acetyl glucosamine and N-acetyl glucosamine-N-acetyl glucosamine linkages. Thus in the presence of lysozyme release of the drug takes place by diffusion followed by enzymatic degradation of the polymer matrix (Kean & Thanou, 2010; Kim et al., 2006). Table 1 shows the percentage of curcumin released from *O*-CMC matrix at different time periods.

3.7. Cytotoxicity assay

Cytotoxicity of *O*-CMC Nps, curcumin and curcumin-*O*-CMC Nps on L929, MCF-7 and PC-3 were studied using MTT assay as shown in Fig. 5. L929 (Fig. 5A) exposed to *O*-CMC Nps showed high cell viability whereas the viability reduced when exposed to curcumin and curcumin-*O*-CMC Nps in the concentration range 1–5 mg/ml. However, 80% of the cells were viable indicating the non-toxicity of curcumin, *O*-CMC Nps and curcumin-*O*-CMC Nps towards normal cells. For MCF-7 (Fig. 5B) *O*-CMC Nps showed no toxicity whereas curcumin and curcumin-*O*-CMC Nps showed considerable toxicity. Similarly in PC-3 (Fig. 5C) curcumin-*O*-CMC Nps showed toxicity as a result of which cell viability reduced to 30% at 5 mg/ml confirming its anticancer effects. Curcumin-*O*-CMC Nps and curucmin showed comparable effect on cancer cells which indicate that curcumin retains its anticancer activity even after being loaded into polymer matrix.

3.8. Cell uptake studies

Cellular uptake studies of curcumin-*O*-CMC Nps were studied by visualizing the intrinsic fluorescence of curcumin using fluorescence microscopy (Fig. 6A). Control cells without any exposure to curcumin and cells incubated with *O*-CMC Nps showed no fluorescence (Fig. 6A (i and j)). Cells incubated with curcumin-*O*-CMC Nps shows green fluorescence confirming the internalization of the particles in the cells. L929 (Fig. 6A (c and d)) treated with 1 and 5 mg/ml and MCF-7 treated with 1 mg/ml curcumin-*O*-CMC Nps (Fig. 6A (g)) have retained its stretched morphology where as MCF-7 cells (Fig. 6A (h)) exposed to 5 mg/ml curcumin-*O*-CMC Nps appeared to be rounded off so as to undergo apoptosis. This confirms the release of curucumin from the Np matrix within the cells and showing its anticancer effects.

3.9. Cell uptake measurements by UV quantification

The cellular uptake of curcumin-*O*-CMC Nps by normal and cancer cells was quantified using ethanol extraction method where the released drug within the cells was measured spectrophotometri-

Table 1
Percentage release of curcumin from *O*-CMC nanoparticles at different time intervals.

Time (h)	Drug released (%) without lysozyme		Drug released (%) with lysozyme	
	pH 7.4	pH 4.5	pH 7.4	pH 4.5
1	3	6	5	10
6	17	22	20	22
12	26	24	29	32
24	33	28	33	40
48	35	38	40	43
72	43	47	52	56
96	51	58	54	60
102	52	59	54	63
126	53	59	59	68

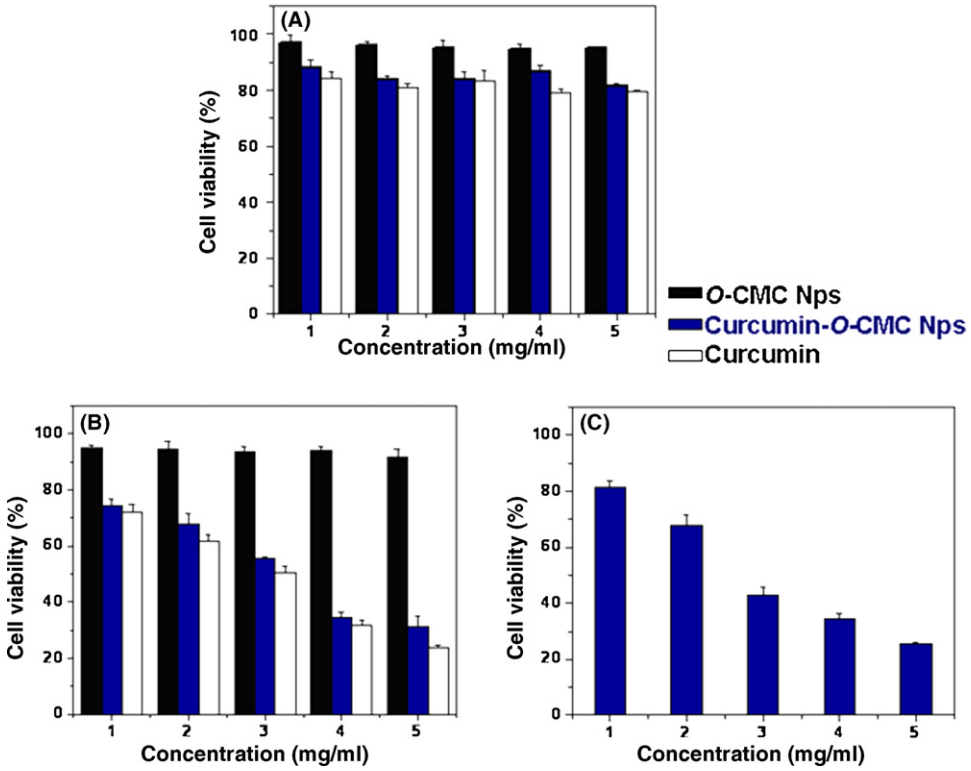

Fig. 5. Cell viability of (a) normal cells (L929) (b) breast cancer cells (MCF-7) and (c) prostate cancer cells (PC-3) treated with *O*-CMC Nps, curcumin and curcumin-*O*-CMC Nps.

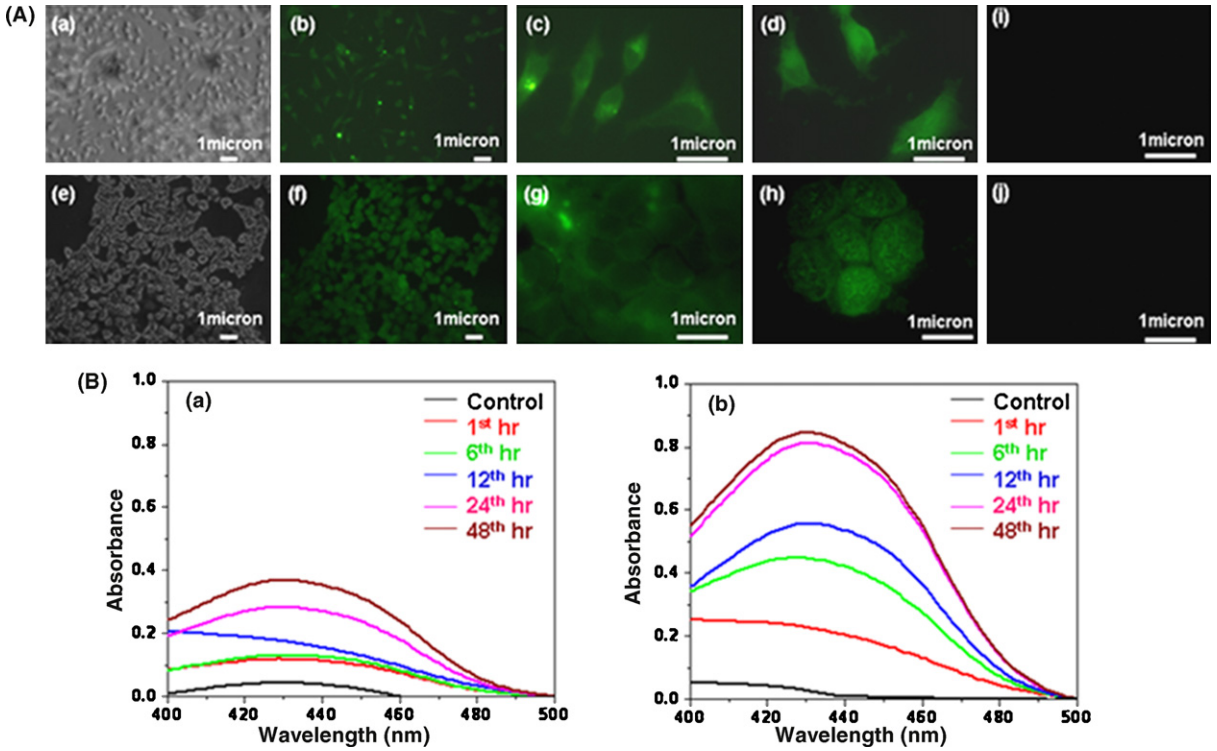

Fig. 6. (A) Fluorescence Images of curcumin-*O*-CMC Nps (a) and (b) bright field and fluorescent image of L929 at 20× (c) and (d) L929 with 1 and 5 mg/ml sample at 100× (e) and (f) bright field and fluorescent image of MCF-7 at 20× (g) and (h) MCF-7 with 1 and 5 mg/ml sample at 100× (i) *O*-CMC Nps (j) control cells alone. (B) Absorbance spectrum of ethanolic curcumin extracted from (a) L929 (b) MCF-7 at different time intervals.

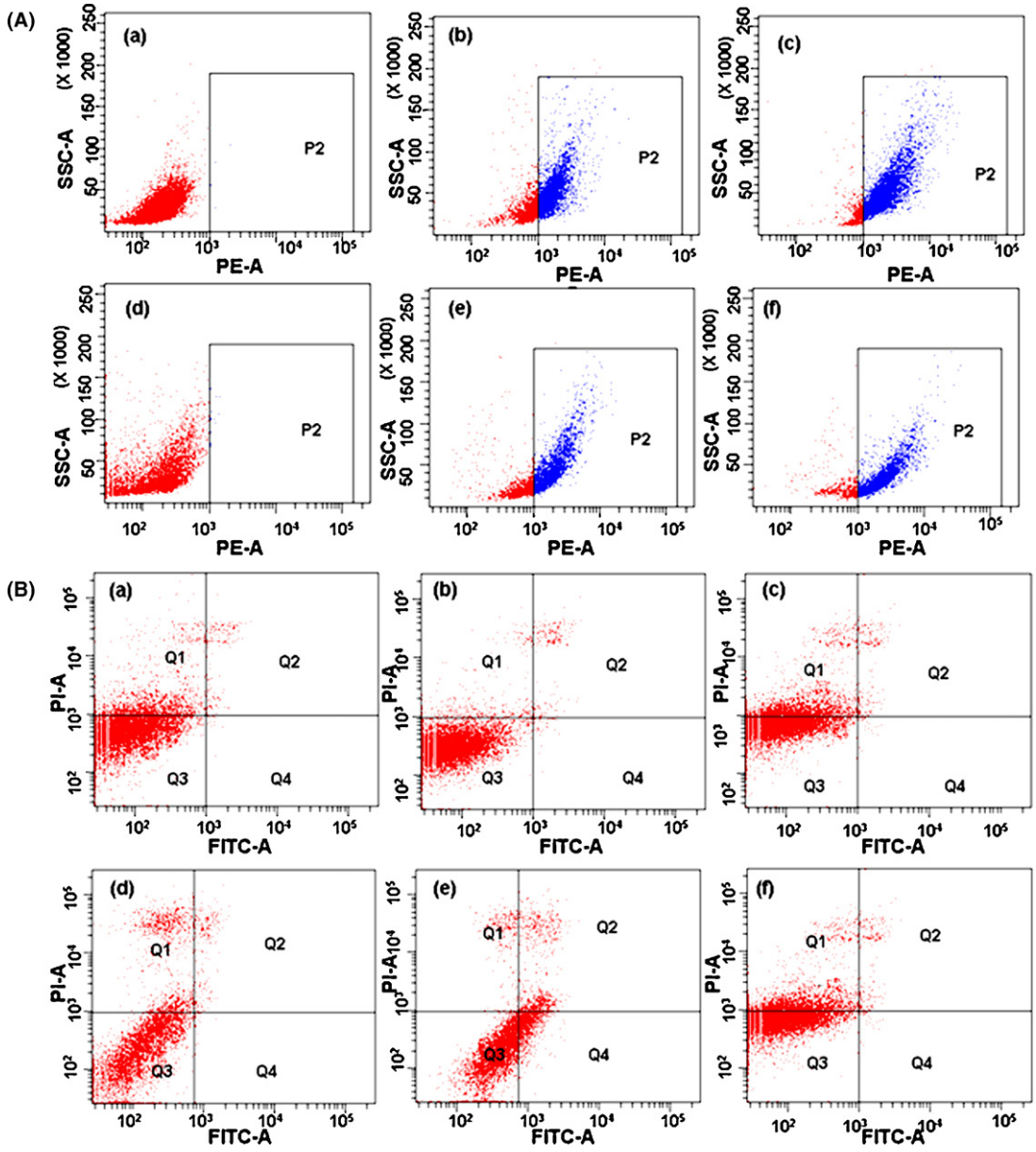

Fig. 7. (A) Cellular uptake of curcumin-*O*-CMC Nps by FACS (a) control L929 cells alone (b) and (c) L929 exposed to 1 and 5 mg/ml curcumin-*O*-CMC Nps (d) control MCF-7 cells alone (e) and (f) exposed to 1 and 5 mg/ml curcumin-*O*-CMC Nps (B) Apoptosis assay by FACS (a) control L929 cells exposed to *O*-CMC Nps (b) and (c) L929 exposed to 1 and 5 mg/ml curcumin-*O*-CMC Nps (d) control MCF-7 cells exposed to *O*-CMC Nps (e) and (f) exposed to 1 and 5 mg/ml curcumin-*O*-CMC Nps.

cally. Fig. 6B (a and b) shows the absorption spectra of ethanolic curcumin extracted from L929 and MCF-7 respectively. It is clear that there was an increased release of drug within MCF-7 compared to L929 with increased in time intervals which can be due to more cellular internalization of curcumin-*O*-CMC Nps or due to increased release of curcumin within cancer cells.

3.10. Cellular uptake by FACS analysis

The cellular uptake of curcumin-*O*-CMC Nps by normal and cancer cells were investigated using flow cytometry. Fig. 7A shows the uptake profile indicating that both the cell lines shows an increased uptake with increasing concentrations of curcumin-*O*-CMC Nps. Comparing normal and cancer cell lines there is not much significant difference in the uptake of particles which can be due to the negative charge of curcumin-*O*-CMC Nps. This result indicated that the cellular uptake of these nanoparticles by the cells is nonspecific and concentration dependant.

3.11. Apoptosis assay by FACS analysis

Fig. 7B shows the apoptotic profile of *O*-CMC Nps and curcumin-*O*-CMC Nps. Cells exposed to *O*-CMC Nps did not show any apoptosis in both cancer cells as well as normal cells. It is evident that the percentages of apoptotic cells observed in case of MCF-7 were more compared to that of L929. Percentage of cells showing apoptosis when exposed to higher concentration (5 mg/ml) of curcumin-*O*-CMC Nps were more than to lower concentration (1 mg/ml). From the data it can be speculated that cancer cells exposed to higher concentration of curcumin-*O*-CMC Nps showed enhanced toxicity due to higher uptake at higher concentration. Even though there is no considerable difference in the uptake of

particles between normal and cancer cells, more apoptosis in cancer cells indicates the release of curcumin within the cancer cells and showing the specific anticancer activity of the drug. This can be due to the fact that curcumin targets the signaling molecules that are highly expressed in cancer cells. In normal cells, these pathways will be regulated and curcumin will arrest the cell division in G0 phase without inducing apoptosis (Sa & Das, 2008).

4. Conclusions

O-CMC Nps were prepared by a simple method and curcumin was effectively loaded into them. Curcumin-*O*-CMC Nps were tuned within the optimum size range suitable for drug delivery application. *In vitro* drug release profile indicated slow, controlled and sustained release of drug from the Np matrix and also demonstrated enzyme triggered degradation and release of the drug in the presence of lysozyme. Fluorescence microscopic image showing green fluorescence confirmed the successful delivery of curcumin from the nanoparticle matrix and its anticancer effect was confirmed by MTT assay. FACS analysis confirmed the cellular uptake of curcumin-*O*-CMC Nps and apoptosis within the cancer cells. These preliminary studies show that *O*-CMC Nps can be a promising candidate for carrying hydrophobic drugs like curcumin making it suitable for cancer drug delivery applications.

Acknowledgments

The authors are thankful to Department of Biotechnology (DBT), Govt. of India, for their financial support for this work under the Nanoscience and Nanotechnology Initiative program (Ref.No.BT/PR10882/NNT/28/142/2008). This work was also partially supported by Nanomission, Department of Science and Technology, India under the Nanoinitiative Program monitored by Prof. C.N.R. Rao. One of the authors A. Anitha is thankful to Council of Scientific and Industrial Research (CSIR), India for providing Senior Research Fellowship (SRF award-Ref.No.9/963 (0005) 2K10-EMR-I) for carrying out her research work. The authors are also thankful to Koyo chemicals Co. Ltd., Japan for providing *O*-CMC. The authors are also thankful to Mr. Sajin. P. Ravi, Mr. Girish, C.M. Mr. Sarath and Mr. Sudheesh Kumar P.T. for their help in SEM, AFM and TG/DTA studies.

References

Anand, P., Sundaram, C., Jhurani, S., Ajaikumar, B., Kunnumakkara, & Aggarwal, B. B. (2008). Curcumin and cancer: An "old age" disease with an "age-old" solution. *Cancer Letters*, *267*, 133–164.

Anitha, A., Divyarani, V. V., Krishna, R., Sreeja, V., Selvamurugan, N., Nair, S. V., et al. (2009). Synthesis, characterization, cytotoxicity and antibacterial studies of chitosan, *O*-carboxymethyl and *N*, *O*-carboxymethyl chitosan nanoparticles. *Carbohydrate Polymers*, *78*, 672–677.

Chen, X. G., & Park, H. J. (2003). Chemical characteristics of *O*-Carboxymethyl chitosan related to its preparation conditions. *Carbohydrate Polymers*, *53*, 355–359.

Cho, K., Wang, X., Nie, S., Chen, Z., & Shin, D. M. (2008). Therapeutic nanoparticles for drug delivery in cancer. *Clinical Cancer Research*, *14*, 1310–1316.

Csaba, N., Koping-Hoggard, M., & Alonso, M. J. (2009). Ionically cross linked chitosan/tripolyphosphate nanoparticles for oligonucleotide and plasmid DNA delivery. *International Journal of Pharmaceutics*, *382*, 205–214.

Das, R. K., Kasoju, N., & Bora, U. (2010). Encapsulation of curcumin in alginate chitosan pluronic composite nanoparticles for delivery to cancer cells. *Nanomedicine: Nanotechnology, Biology and Medicine*, *6*, 153–160.

Dev, A., Jithin, C. M., Sreeja, V., Tamura, H., Patzke, G. R., Hussain, F., et al. (2010). Novel carboxymethyl chitin nanoparticles for cancer drug delivery applications. *Carbohydrate Polymers*, *79*, 1073–1079.

Fernando, R. D. A., & Sergio, P. C. (2004). Characteristics and properties of carboxymethyl chitosan related to preparation conditions. *Carbohydrate Polymers*, *75*, 214–221.

Gelperina, S., Kisich, K., Iseman, M. D., & Heifets, L. (2005). The potential advantages of nanoparticle drug delivery systems in chemotherapy of tuberculosis. *American Journal of Respiratory and Critical Care Medicine*, *172*, 1487–1490.

Jayakumar, R., Nair, S. V., & Tamura, H. (2009). Biomedical applications of chitin. *Asian Chitin Journal*, *5*, 1–4.

Jayakumar, R., Chennazhi, K. P., Muzzarelli, R. A. A., Tamura, H., Nair, S. V., & Selvamurugan, N. (2010). Chitosan conjugated DNA nanoparticles in gene therapy. *Carbohydrate Polymers*, *79*, 1–8.

Jayakumar, R., Prabaharan, M., Nair, S. V., Tokura, S., Tamura, H., & Selvamurugan, N. (2010). Novel carboxymethyl derivatives of chitin and chitosan materials and their biomedical applications. *Progress in Materials Science*, *55*, 675–709.

Jung, T., Kamm, W., Breitenbach, A., Kaiserling, E., Xiao, J. X., & Kissel, T. (2000). Biodegradable nanoparticles for oral delivery of peptides: Is there a role for polymers to affect mucosal uptake. *European Journal of Pharmaceutical Sciences*, *50*, 147–160.

Karikar, C., Maitra, A., Bisht, S., Feldmann, G., Soni, S., & Ravi, R. (2007). Polymeric nanoparticle-encapsulated curcumin ("nanocurcumin"): a novel strategy for human cancer therapy. *Journal of Nanobiotechnology*, *5*, 3–21.

Kean, T., & Thanou, M. (2010). Biodegradation, biodistribution and toxicity of chitosan. *Advanced Drug Delivery Reviews*, *62*, 3–11.

Khan, T. A., Peh, K. K., & Chng, H. S. (2000). Mechanical, bioadhesive strength and biological evaluations of chitosan films for wound dressing. *Journal of Pharmacy and Pharmaceutical Sciences*, *3*, 303–311.

Khor, E, & Lim, L. Y. (2003). Implantable applications of chitin and chitosan. *Biomaterials*, *24*, 2339–2349.

Kim, D. G., Jeong, Y. I., Choi, C., Roh, S. H., Kang, S. K., Jang, M. K., et al. (2006). Retinol-encapsulated low molecular water-soluble chitosan nanoparticles. *International Journal of Pharmaceutics*, *319*, 130–138.

Kumar, V., Lewis, S. A., Mutalik, S., Shenoy, D. B., Venkatesh, & Udupa, N. (2002). Biodegradable microspheres of curcumin for the treatment of inflammation. *Indian Journal of Physiology and Pharmacology*, *46*, 209–217.

Kunwar, A., Barik, A., Mishra, B., Rathinasamy, K., Pandey, R., & Priyadarshini, K. I. (2008). Quantitative cellular uptake, localization and cytotoxicity of curucmin in normal and tumor cells. *Biochimica et Biophysica Acta*, *1780*, 673–679.

Lao, C. D., Demierre, M. F., & Sondak, V. K. (2006). Targetting events in melanoma carcinogenesis. *Anticancer Therapy*, *6*, 1559–1568.

Li, L., Ahmed, B., Mehta, K., & Kurzrock, R. (2007). Liposomal curcumin with and without oxaliplatin: Effects on cell growth, apoptosis, and angiogenesis in colorectal cancer. *Molecular Cancer Therapeutics*, *6*, 1276–1282.

Liu, X. F., Guan, Y. L., Yang, D. Z., Li, Z., & Yao, K. D. (2001). Antibacterial action of chitin and carboxymethylated chitosan. *Journal of Applied Polymer Science*, *79*, 1324–1335.

Madhumathi, K., Sudheesh Kumar, P. T., Abhilash, S., Sreeja, V., Tamura, H., Manzoor, K., et al. (2010). Development of novel chitin/nanosilver composite scaffolds for wound dressing applications. *Journal of Materials Science: Materials in Medicine*, *21*, 807–813.

Mathew, E. M., Jithin, C. M., Manzoor, K., Nair, S. V., Tamura, H., & Jayakumar, R. (2010). Folate conjugated carboxymethyl chitosan-manganese doped zinc sulphide nanoparticles for targeted drug delivery and imaging of cancer cells. *Carbohydrate Polymers*, *80*, 442–448.

Mishra, V. K., Mohammada, G., & Mishra, S. K. (2008). Downregualation of telomerase activity may enhanced by nanoparticle mediated curcumin delivery. *Digest Journal of Nanomaterials and Biostructures*, *3*, 163–169.

Muller, R. H., & Keck, C. M. (2004). Challenges and solutions for the delivery of Biotech drugs – a review of drug nanocrystal technology and lipid nanoparticles. *Journal of Biotechnology*, *113*, 151–155.

Muzzarelli, R. A. A., Ramos, V., Stanic, V., Dubini, B., Mattioli-Belmonte, M., Tosi, G., et al. (1998). Osteogenesis promoted by calcium phosphate *N*, *N*-dicarboxymethyl chitosan. *Carbohydrate Polymers*, *36*, 267–276.

Peter, M., Ganesh, N., Selvamurugan, N., Nair, S. V., Furuike, T., Tamura, H., et al. (2010). Preparation and characterization of chitosan-gelatin/nanohydroxyapatite composite scaffolds for tissue engineering applications. *Carbohydrate Polymers*, *80*, 687–694.

Pfeiffer, E., Hohle, S., Solyom, A., & Metzler, M. (2003). Study of turmeric constituents. *Journal of Food Engineering*, *56*, 257–259.

Prabaharan, M., Reis, R. L., & Mano, J. F. (2007). Carboxymethyl chitosan-*graft*-phosphatidylethanolamine: Amphiphilic matrices for controlled drug delivery. *Reactive and Functional Polymers*, *67*, 43–52.

Qureshi, S., Shah, A. H., & Ageel, A. M. (1992). Toxicity studies on *Alpinia galanga* and *Curcuma longa*. *Planta Medica*, *58*, 124–127.

Rabea, E. I., Badawy, M. E., Stevens, C. V., Smagghe, G., & Steubaut, W. (2003). Chitosan as antimicrobial agent: Applications and mode of action. *Biomacromolecules*, *4*, 1457–1465.

Sa, G., & Das, T. (2008). Anticancer effects of curcumin: cycle of life and death. *Cell Division*, *3*(14) doi:10.1186/1747-1028r-r3-14

Salmaso, S., Bersani, S., Semenzato, A., & Caliceti, P. (2007). New cyclodextrin bioconjugates for active tumor targeting. *Journal of Drug Targeting*, *15*, 379–390.

Sou, K., Inenaga, S., Takeoka, S., & Tsuchida, E. (2007). Loading of curcumin into macrophages using lipid-based nanoparticles. *International Journal of Pharmaceutics*, *352*, 287–293.

Shankar, T. N., Shantha, N. V., Ramesh, H. P., Murthy, I. A., & Murthy, V. S. (1980). Toxicity studies on turmeric: Acute toxicity studies in rats, guinea pigs and monkeys. *Indian Journal of Experimental Biology*, *18*, 73–75.

Shaikh, J., Ankola, D. D., Beniwal, V., Singh, D., & Ravikumar, M. N. V. (2009). Nanoparticle encapsulation improves oral bioavailability of curcumin by atleast 9-fold when compared to curcumin administered with piperine as absorption enhancer. *European Journal of Pharmaceutical Sciences*, *37*, 223–230.

Shi, X., Du, Y., Yang, J., Zhang, B., & Sun, L. (2006). Effect of degree of substitution and molecular weight of carboxymethyl chitosan nanoparticles on doxorubicin delivery. *Journal of Applied Polymer Science*, *100*, 4689–4696.

Sudheesh Kumar, P. T., Abhilash, S., Manzoor, K., Nair, S. V., Tamura, H., & Jayakumar, R. (2010). Preparation and characterization of novel β-chitin/nanosilver composite scaffolds for wound dressing applications. *Carbohydrate Polymers*, *80*, 761–767.

Tiyaboonchai, W., Tungpradit, W., & Plianbangchang, P. (2007). Formulation and characterization of curcuminoids loaded solid lipid nanoparticles. *International Journal of Pharmaceutics*, *337*, 299–306.

Vemula, P. K., Li, J., & John, G. (2006). Enzyme catalysis: Tool to make and break amygdalin hydrogelators from renewable resources: A delivery model for hydrophobic drugs. *Journal of American Chemical Society*, *128*, 8932–8938.

Wang, Y. J., Pan, M. H., Cheng, A. L., Lin, L. I., & Lin, J. K. (1997). Stability of curcumin in buffer solutions and characterization of its degradation products. *Journal of Pharmaceutical and Biomedical Analysis*, *15*, 1867–1876.

Wang, X. H., Du, Y. M., Fan, L. H., Liu, H., & Hu, Y. (2005). Chtiosan-metal complexes as antimicrobial agent: synthesis and characterization and structure-activity study. *Polymer Bulletin*, *55*, 105–113.

Yallapua, M. M., Jaggi, M., & Chauhana, S. C. (2010). β-Cyclodextrin-curcumin self-assembly enhances curcumin delivery in prostate cancer cells. *Colloids and Surfaces B*, *79*, 113–125.

Zhuang, X. P., & Liu, X. F. (2006). Blend films of *O*-carboxymethyl chitosan and cellulose in *N*-methylmorpholine-*N*-oxide monohydrate. *Journal of Applied Polymer Science*, *102*, 4601–4605.